



PAPER

Narrowband noise study of sliding charge density waves in NbSe₃ nanoribbons

OPEN ACCESS

RECEIVED

4 October 2016

REVISED

9 January 2017

ACCEPTED FOR PUBLICATION

12 January 2017

PUBLISHED

1 February 2017

Original content from this work may be used under the terms of the [Creative Commons Attribution 3.0 licence](#).

Any further distribution of this work must maintain attribution to the author(s) and the title of the work, journal citation and DOI.

Seita Onishi^{1,2,3}, Mehdi Jamei^{1,2,3} and Alex Zettl^{1,2,3}¹ Department of Physics, University of California at Berkeley, Berkeley, CA 94720, United States² Materials Sciences Division, Lawrence Berkeley National Laboratory, Berkeley, CA 94720, United States³ Kavli Energy NanoSciences Institute at the University of California Berkeley and the Lawrence Berkeley National Laboratory, Berkeley, CA 94720, United StatesE-mail: azettl@berkeley.edu**Keywords:** sliding charge density wave, niobium triselenide, nanoribbon, narrowband noiseSupplementary material for this article is available [online](#)

Abstract

Transport properties (dc electrical resistivity, threshold electric field, and narrow-band noise) are reported for nanoribbon specimens of NbSe₃ with thicknesses as low as 18 nm. As the sample thickness decreases, the resistive anomalies characteristic of the charge density wave (CDW) state are suppressed and the threshold fields for nonlinear CDW conduction apparently diverge. Narrow-band noise measurements allow determination of the concentration of carriers condensed in the CDW state n_c , reflective of the CDW order parameter Δ . Although the CDW transition temperatures are relatively independent of sample thickness, in the lower CDW state Δ decreases dramatically with decreasing sample thickness.

1. Introduction

Low dimensional charge density wave (CDW) materials have enjoyed a resurgence of research popularity driven largely by interest in two-dimensional materials in the ultrathin limit. Layered transition metal dichalcogenides (MX₂), which in the bulk often support CDW collective mode ground states, can be exfoliated [1] to yield ultrathin specimens down to the monolayer. Examples include TiSe₂ [2], TaS₂ [3, 4] and NbSe₂ [5, 6]. In contrast, transition metal trichalcogenides (MX₃) are CDW-supporting materials consisting of weakly bonded one-dimensional chains [7, 8]. Remarkably, the CDW in MX₃ materials is often found to be *dynamic*, where the collective mode oscillating about impurity pinning centers yields strongly frequency dependent ac conductivity at relatively low (e.g. MHz) frequencies, and, even more spectacularly, enhanced dc conductivity reflecting a ‘sliding’ CDW condensate for applied dc electric fields exceeding a small threshold field E_T [9]. Of special interest is the behavior of the CDW state of dynamic CDW systems as the sample dimensions become much less than the transverse phase correlation length, ultimately approaching the single chain limit.

The prototype incommensurate sliding CDW MX₃ material NbSe₃ has two independent CDW states, the first setting in at $T_{P1} = 144$ K and the second at $T_{P2} = 59$ K [10]. Independent resistive anomalies are observed below T_{P1} and T_{P2} , associated with partial gapping of the Fermi surface. CDWs in NbSe₃ have a transverse phase correlation length on the order of $l \sim 1 \mu\text{m}$ [11]. Preliminary studies [12–16] of dimensionally reduced NbSe₃ nanowires and nanoribbons indicate that both T_{P1} and T_{P2} appear to have only a slight dependence on sample size. On the other hand, E_T increases, and the CDW resistive anomalies are strongly reduced, with decreasing sample size. No studies have reported the dependence of the CDW order parameter on sample size.

We here report on transport and narrowband noise measurements on mechanically cleaved thin samples of NbSe₃, down to thicknesses of 18 nm. The relative insensitivity of T_P , increase of E_T , and suppression of the resistive anomalies, with decreasing sample size are confirmed. Narrowband noise measurements in the lower CDW state show that the CDW order parameter Δ decreases markedly with decreasing sample size. The low frequency dielectric constant ϵ_1 is found to be strongly sample size dependent.

Table 1. NbSe₃ nanoribbon sample parameters. NbSe₃ sample dimensions (thickness, width and length) and two-probe resistances at room temperature are displayed. The contact resistance is calculated from comparison with bulk conductivity of $2.5 \times 10^{-4} \Omega \text{ cm}$ [9].

Sample #	Thickness (nm)	Width (nm)	Length (μm)	Resistance at RT (k Ω)	Contact resistance (%)
1	55	550	7.4	0.76	19.5
2	34	450	4.6	0.92	18.3
3	31	280	3.2	1.08	14.6
4	18	150	1.1	1.20	15.1

2. Experimental

High-purity NbSe₃ crystals with typical dimensions $1 \mu\text{m} \times 10 \mu\text{m} \times 1 \text{ cm}$ initially grown by chemical vapor transport are thinned down by mechanical exfoliation using the Scotch tape method [1], and then deposited on a Si/SiO₂ substrate. Previous studies report preparation of NbSe₃ nanowires by ultrasonic cleaving [16], direct synthesis [17, 18], or plasma etching [19]. We find that mechanical exfoliation is the most reliable method to prepare undamaged samples of NbSe₃ of different thicknesses having consistent impurity concentration. The sample dimensions post-cleaving are determined using a combination of optical microscopy, scanning electron microscopy, and atomic force microscopy.

Table 1 summarizes the dimensions of the samples discussed in this report. Cleaved samples have thickness t equal to 55, 34, 31, and 18 nm. Sample widths and lengths are approximately $10t$ and $100t$, respectively (see table 1 for details). The sample length is defined as the distance between electrical contacts, not the overall physical length of the crystallite. We find that the conventional method of electrical contact to NbSe₃ via conductive silver paint is unreliable for ultrathin samples. Instead, In/Cr/Au trilayer contacts are placed on the NbSe₃ crystal employing electron beam lithography and metal evaporation. Immediately prior to electrode evaporation, the sample is treated with nitrogen plasma, a key to low contact resistance. Plasma treatment is limited only to the contacts locations and the active area of the sample is protected by electron beam resist. Our careful comparisons between two- and four-probe contact configurations on selected thin samples indicate that the contact resistance is relatively low. Therefore, for transport and noise measurements here reported, a two-probe contact configuration is employed. Table 1 lists electrical resistance at room temperature for the different samples, and worst-case estimates for contact resistances. The samples are cooled in a helium gas environment using a home-made gas flow cryostat.

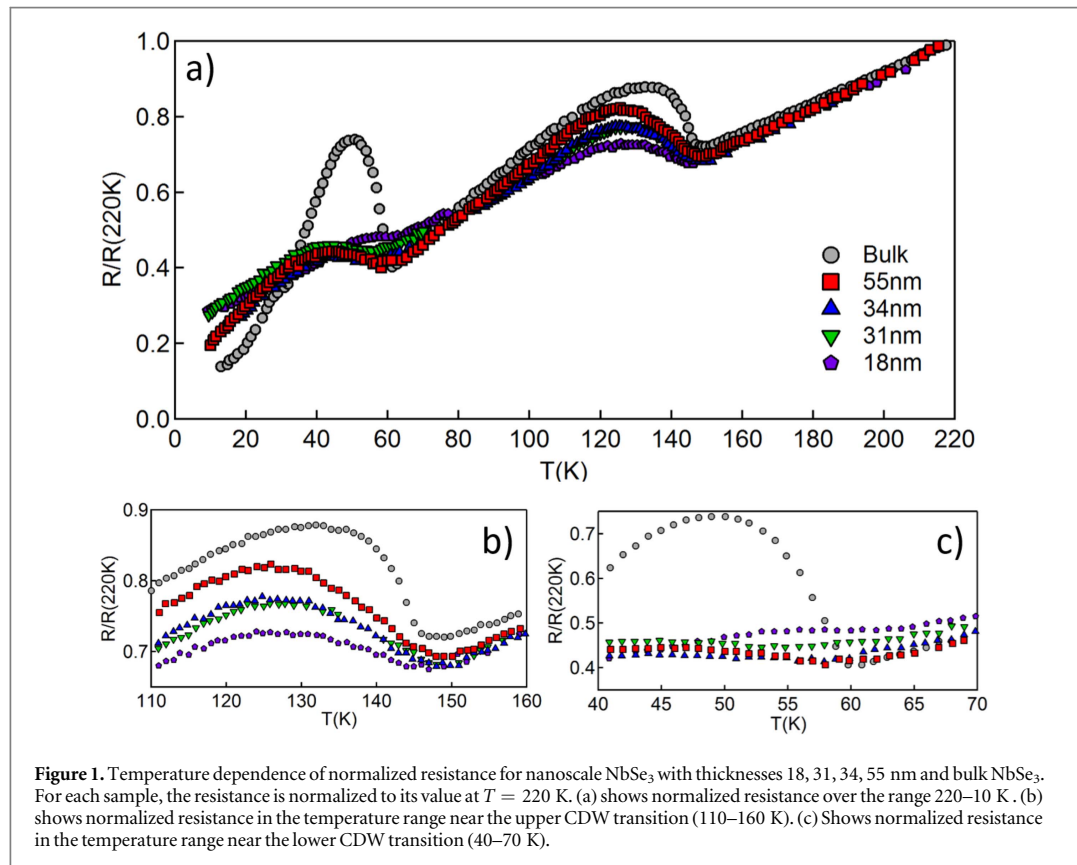
3. Results and discussion

Figure 1(a) shows the normalized dc electrical resistance R of NbSe₃ samples in the temperature range 220–10 K. In order to compare samples of different thicknesses, the resistance for each sample is normalized by its resistance at 220 K. The samples are current biased at low excitation to remain below the threshold field for nonlinear conduction. The temperature dependence of resistance is overall metallic except for the two well-known upturns, starting at $T_{p1} = 144 \text{ K}$ and $T_{p2} = 59 \text{ K}$, corresponding to the upper and lower CDW transitions, respectively. The recovery of metallic behavior below the resistance anomalies is attributed to incomplete gapping of the Fermi surface [10]. Figures 1(b) and (c) show details of the normalized resistance near T_{p1} and T_{p2} , respectively. Previous studies [16] have indicated that both CDW transition temperatures in NbSe₃ have a modest dependence on sample size, with T_p decreasing with decreasing size. Our $R(T)$ data of figures 1(b), (c) (plotted as $(1/R)dR/dT$ versus T , see supplementary material figures S1(a), (b))⁴, are not inconsistent with this assertion (with our data suggesting T_{p1} decreases from 144 K for bulk samples to 140 K for the 18 nm sample), but our large experimental error bars make it difficult to identify an unambiguous trend, especially for T_{p2} . In any case, and perhaps not surprisingly (considering the 1D nature of the material), T_p is not very sensitive to sample size in NbSe₃.

Figure 1 shows that the resistive anomalies in NbSe₃ are dramatically suppressed with decreasing sample size, as reported in previous studies [16, 18]. The lower CDW state is particularly sensitive, with the resistive anomaly below $T_{p2} = 59 \text{ K}$ severely suppressed (but still detectable, see supplementary material figures S2(a)–(d))⁵ for the 18 nm sample. In contrast, the upper CDW resistive anomaly is suppressed by only $\sim 50\%$ for the 18 nm sample. The significant difference in size sensitivity between the lower and upper CDW states has not been observed in earlier studies of NbSe₃ nanowires produced by ultrasonic cleaving [16]. We attribute the difference

⁴ See supplemental material at (URL will be inserted by publisher) for T_{p1} and T_{p2} determined by numerical derivatives of $R(T)$.

⁵ See supplemental material at (URL will be inserted by publisher) for $R(T)$ in figure 1(c) with each curve isolated in a separate panel for clarity. The CDW resistive anomaly is small but detectable for thicknesses between 55 and 18 nm.

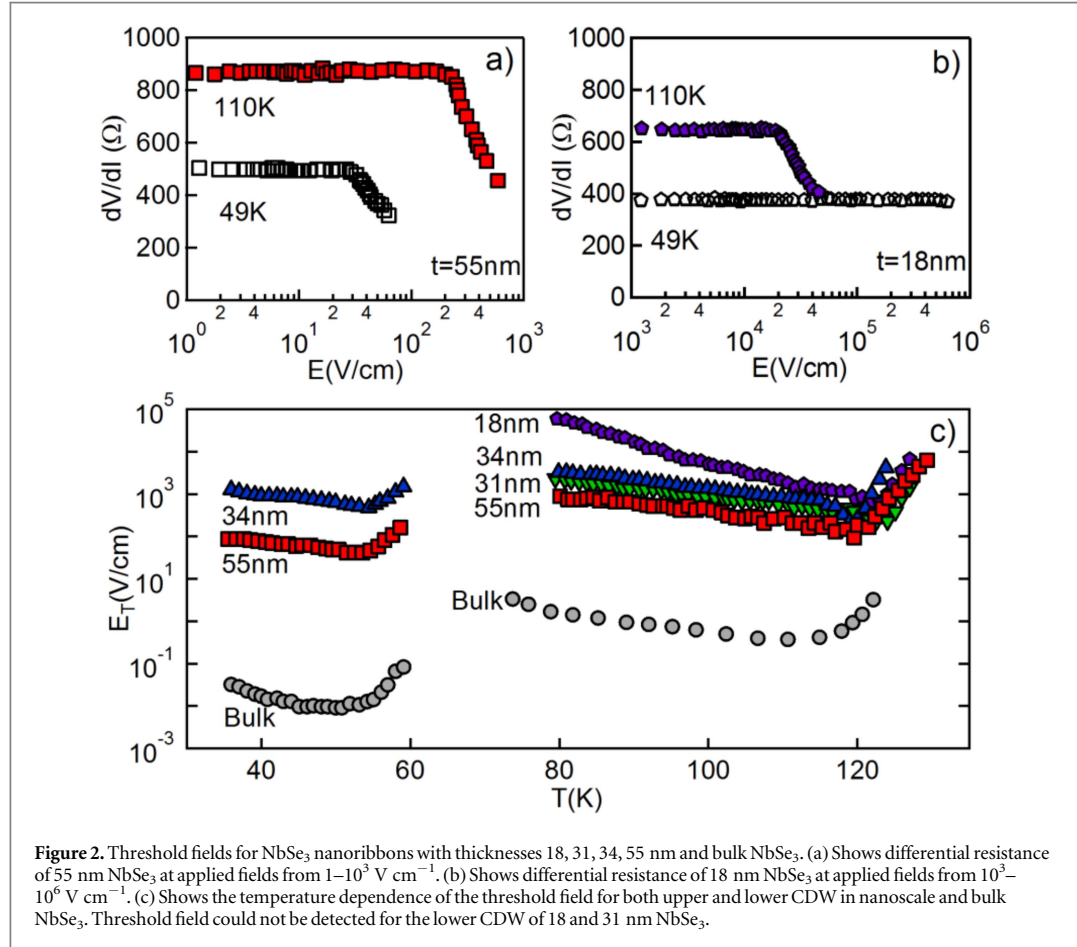


to the width-to-thickness ratio (w/t) of the samples. Our ribbon-like samples have $w/t \sim 10$ (table 1), whereas the nanowires in the earlier study have $w/t \sim 1$. Even for the thinnest (18 nm) nanoribbon sample, R continues to exhibit metallic behavior (i.e. decreasing R with decreasing T) at low temperature. These findings are in contrast to earlier NbSe₃ nanowire studies [16], where for thin samples non-metallic one-dimensional power law behavior ($R \sim T^{-\alpha}$) was observed at low temperature.

We now examine the dynamic CDW sliding state and thereby gain insight into the CDW order parameter. The threshold field E_T for the onset of CDW sliding conduction is obtained at fixed temperature either from low frequency differential resistance measurements or pulsed methods. The differential resistance $R_{\text{diff}} = dV/dI$ is measured by a lock-in amplifier employing a 0.01 nV excitation at 500 Hz. Pulse methods, which avoid heating at high applied E , use a 1 μs pulse width and low duty cycle [20].

Figures 2(a) and (b) show R_{diff} vs applied electric field E for the 55 nm and 18 nm NbSe₃ nanoribbons, respectively. In the upper CDW state at 110 K, where $E_T(\text{bulk}) = 0.2 \text{ V cm}^{-1}$, E_T for the 55 nm sample is 196 V cm^{-1} , while for the 18 nm sample it is $20\,000 \text{ V cm}^{-1}$. In the lower CDW state at 49 K, where $E_T(\text{bulk}) = 0.01 \text{ V cm}^{-1}$, E_T for the 55 nm sample is 28 V cm^{-1} , while for the 18 nm sample no depinning is observed for fields as high as $\sim 10^6 \text{ V cm}^{-1}$. Figure 2(c) summarizes E_T behavior for both CDW states for different sample thicknesses. For both CDW states, the same trend is observed: E_T increases with decreasing sample size. This trend is consistent with previous studies [12, 16–18]. For bulk NbSe₃, E_T is typically lower for the lower CDW than the upper CDW [21]. The dependence of E_T on sample size is more acute in the lower CDW state, similar to the high sensitivity on sample size of the lower CDW state resistive anomaly, as described above. For the lower CDW state, E_T apparently diverges to $>10^6 \text{ V cm}^{-1}$ at $t = 18 \text{ nm}$, whereas for the upper CDW state, such a divergence is absent in agreement with the results of a previous study of E_T in the upper CDW state for thin NbSe₃ samples [15]. Comparison of E_T in the upper CDW and lower CDW state for $50 \text{ nm} \leq t \leq 21 \mu\text{m}$ has shown that the E_T temperature dependence is impacted differently by thickness reduction [12]. It is possible that thermal fluctuations influence pinning differently for the upper CDW and the lower CDW.

An interesting question thus arises: in the lower CDW state, is the apparent divergence in E_T with decreasing sample size due to an enhancement in the pinning potential, or due to a rapid collapse in the CDW order parameter? We gain access to the CDW order parameter Δ via narrowband noise measurements. Δ is directly



related to the concentration of carriers condensed in the CDW state⁶ [22], n_c , which is in turn related to the noise frequency f_{NBN} by [23]

$$I_{\text{CDW}} = en_c A \bar{\lambda} f_{\text{NBN}}, \quad (1)$$

where I_{CDW} is the excess current carried by the sliding CDW, e is the electron charge, A is the cross sectional area of the NbSe₃ sample, and $\bar{\lambda}$ is the period of the pinning potential.

To determine f_{NBN} , samples are held at fixed temperature $T = 49$ K in the lower CDW state and dc current biased with $E > E_T$. $I_{\text{CDW}} = I \left(1 - \frac{R}{R_0}\right)$ is extracted from R_0 , the resistance at $E < E_T$. The response voltage is amplified by a custom wideband amplifier and input to a spectrum analyzer. Contact effects from two-point probes are considered negligible⁷ [24]. Figure 3 shows f_{NBN} versus CDW current density $J_{\text{CDW}} = I_{\text{CDW}}/A$ for samples of thickness 34, 55 nm, and bulk. All samples exhibit a linear relation consistent with equation (1). The slopes are used to extract the change in carrier density n_c . Narrowband noise clearly reveals that the lower CDW state order parameter is progressively suppressed as NbSe₃ nanoribbons are thinned. Compared to the bulk, n_c is reduced by more than a factor of five in 34 nm thick NbSe₃, as shown in table 2.

Figure 4(a) summarizes the E_T and n_c behavior as a function of sample thickness t . The different sensitivities of E_T for the upper and lower CDW states leads to a crossing of the $E_T(t)$ curves at ~ 43 nm. Compared to bulk NbSe₃, n_c (and hence Δ) for the lower CDW state is reduced to $0.4n_{c,\text{Bulk}}$ at $t = 55$ nm and decreases further to $0.19n_{c,\text{Bulk}}$ in a thinner sample of $t = 34$ nm. E_T for the lower CDW state is 500 V cm⁻¹ at $t = 34$ nm, and, if it exists at all, exceeds 10^6 V cm⁻¹ at $t = 18$ nm, which is a much steeper increase compared to the upper CDW state. The strength of electric field coupling to the CDW condensate ($F_{\text{CDW}} = e\rho E$) depends on the condensate

⁶ This result supercedes earlier derivations which show $n_c \approx \Delta^2$ near T_p (see for example, [22]). The discrepancy is discussed by Lee and Rice.

⁷ From x-ray measurements [24], it is known that the CDW is strained due to confinement by the contacts for contact separations < 2 nm. From table 1, the contact separations in our samples range from 7.4 to 1.1 nm. However, a multi-contact study [19] has shown that current conversion to the CDW at the contacts is complete and independent of contact spacing from 20 to 0.5 μm .

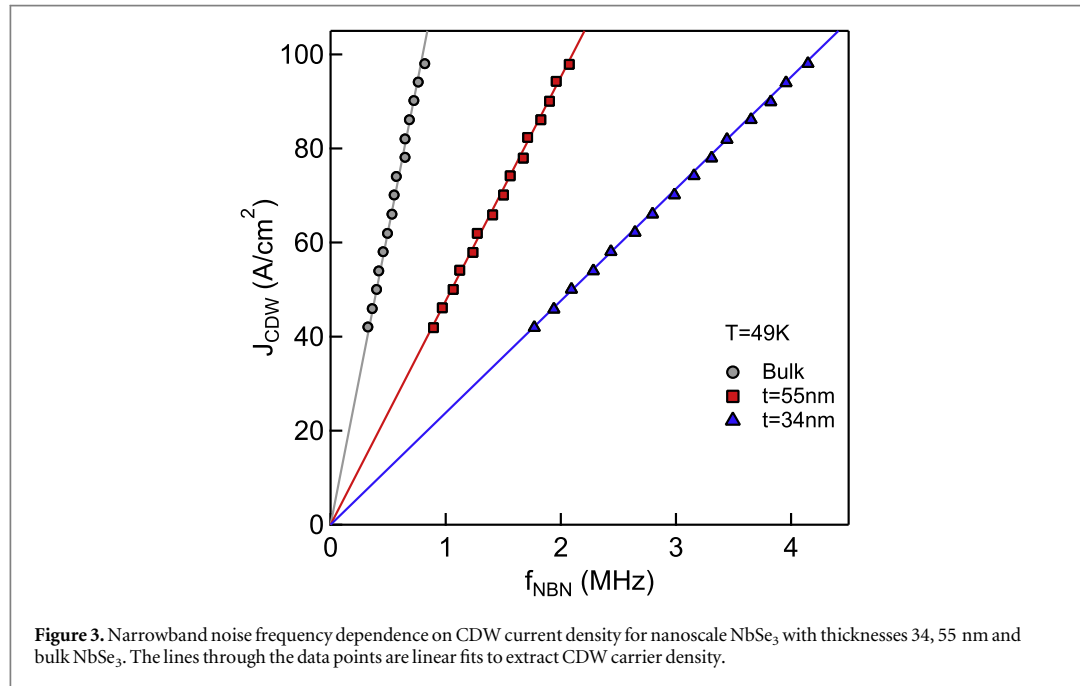


Table 2. CDW parameters of NbSe₃ samples. $E_T(\text{min})$ corresponds to the minimum threshold fields of the upper CDW and lower CDW from the threshold field temperature dependence in figure 2(c). The slope and $n_c/n_{c,\text{Bulk}}$ under 'Lower CDW' are extracted from the linear fit to the measurement of the lower CDW narrowband noise shown in figure 3. The dielectric constant $\varepsilon_1/\varepsilon_{\text{Bulk}}$ are calculated from E_T and n_c at $T = 49$ K. Note1: No E_T found to 10^6 V cm⁻¹.

Sample thickness (nm)	Upper CDW		Lower CDW		
	$E_T(\text{min})$ (V cm ⁻¹)	$E_T(\text{min})$ (V cm ⁻¹)	Slope (A MHz cm ⁻²)	$\frac{n_c}{n_{c,\text{Bulk}}}$	$\varepsilon_1/\varepsilon_{\text{Bulk}}$
Bulk	0.40	0.01	125	1	1
55	100	40	47.6	0.40	7.2×10^{-5}
34	200	500	23.8	0.19	2.7×10^{-6}
31	200	Note 1			
18	800	Note 1			

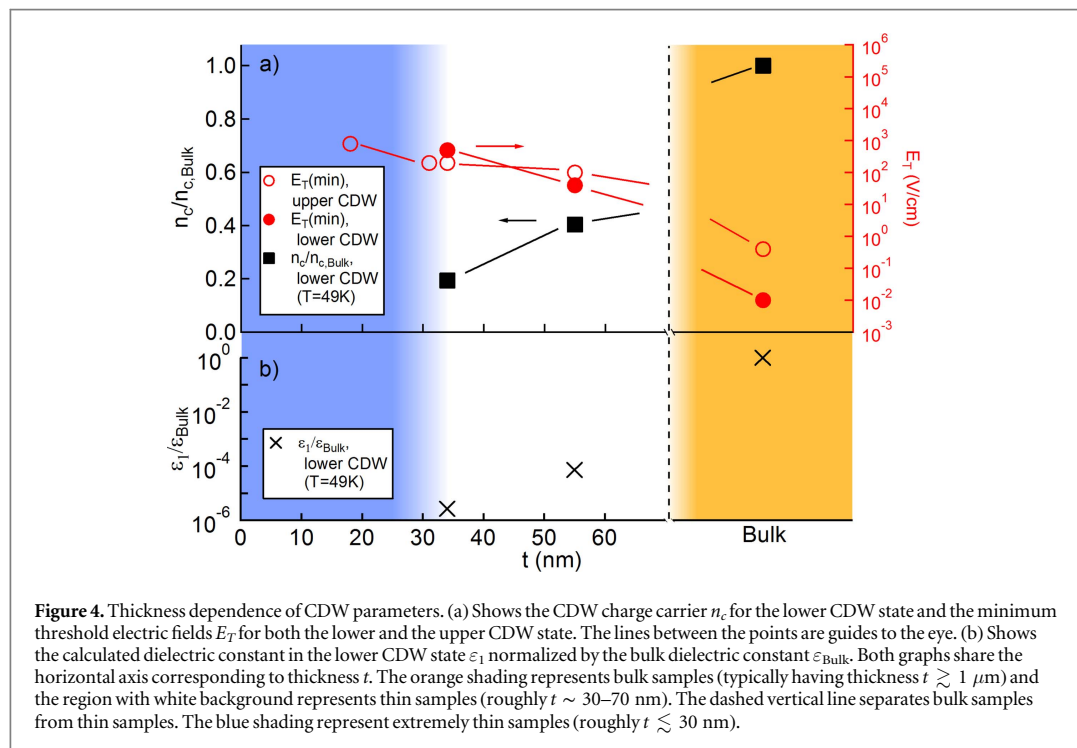
density (ρ), which is determined from Δ [12]. Hence, a strong possibility is that the apparent divergence in E_T is caused by the decrease of the CDW order parameter Δ .

For a CDW system the dielectric constant ε_1 is related to E_T through the expression [9]

$$\varepsilon_1 E_T = (\text{const}) n_c e \bar{\lambda}, \quad (2)$$

where the term (const) is a constant of order one. ε_1 can thus be expressed as $\varepsilon_1(t) \sim n_c(t) e \bar{\lambda} / E_T(t)$ where the size dependences of the relevant parameters are explicitly indicated. With $E_T(t)$ and $n_c(t)$ experimentally determined, $\varepsilon_1(t, T = 49 \text{ K})$ is obtained, as shown in figure 4(b). The low frequency dielectric constant ε_1 at $t = 55$ nm is reduced compared to the bulk and further decreases to 2.7×10^{-6} of $\varepsilon_{\text{Bulk}}$ at $t = 34$ nm. The suppression of the CDW condensate order parameter is expected to result in the suppression of the low frequency dielectric constant ε_1 .

Another possibility for the change in $J_{\text{CDW}}/f_{\text{NBN}}$ is the reduction of effective cross section for thinner samples. We have computed the area ($A = \text{width} \times \text{thickness}$) from sample dimensions listed in table 1. For strong pinning, plasticity in the CDW could lead to a reduced effective cross section compared to the cross section based on sample dimensions [25]. In particular, for surface pinning, the reduction in effective cross section becomes more acute for smaller samples. Hence, the increase of E_T and decrease of $J_{\text{CDW}}/f_{\text{NBN}}$ in thin samples could be due to enhanced surface pinning. As discussed in [12], further study on the shape of narrowband noise spectrum, small-signal ac conductivity, and broadband noise could elucidate the effect of pinning strength distribution and the size dependence of the effective cross section.



4. Conclusion

The sliding CDW in NbSe₃ is investigated for thicknesses from 55 to 18 nm, and the effect of nanoscale confinement on the CDW narrowband noise has been investigated for the first time. At sample thicknesses below $t \sim 30 \text{ nm}$, the lower CDW E_T apparently diverges to $E_T > 10^6 \text{ V cm}^{-1}$, in contrast to the upper CDW E_T which increases at a slower rate with reduced thickness. The difference in size sensitivity between the lower and upper CDW state may be characteristic to ribbon-like samples with $w/t \sim 10$. The results imply that, as NbSe₃ nanoribbons are made thinner, either the CDW order parameter is suppressed or the effective cross section reduces from increased surface pinning. The exploration of CDW dynamics in ultra-thin samples helps illuminate nanoscale confinement effects on CDW materials.

Acknowledgments

Research supported in part by the Director, Office of Science, Office of Basic Energy Sciences, Materials Sciences and Engineering Division, of the US Department of Energy (DOE), under Contract DE-AC02-05CH11231 within the sp²-bonded Materials Program KC2207 (device fabrication); and under an LDRD grant (crystal characterization); by National Science Foundation under award# DMR-1206512 (transport), and EFRI-2DARE grant # 1542741 (synthesis).

References

- [1] Novoselov K S, Jiang D, Schedin F, Booth T J, Khotkevich V V, Morozov S V and Geim A K 2005 *Proc. Natl Acad. Sci. USA* **102** 10451–3
- [2] Goli P, Khan J, Wickramaratne D, Lake R K and Balandin A A 2012 *Nano Lett.* **12** 5941–5
- [3] Yu Y et al 2015 *Nat. Nanotechnol.* **10** 270–6
- [4] Yoshida M, Suzuki R, Zhang Y, Nakano M and Iwasa Y 2015 *Sci. Adv.* **1** e1500606
- [5] Ugeda M M et al 2015 *Nat. Phys.* **12** 92–7
- [6] Xi X, Zhao L, Wang Z, Berger H, Forró L, Shan J and Mak K F 2015 *Nat. Nanotechnol.* **10** 765–9
- [7] Meerschaut A and Rouxel J 1975 *J. Less Common Met.* **39** 197–203
- [8] Roucau C, Ayroles R, Monceau P, Guemas L, Meerschaut A and Rouxel J 1980 *Phys. Status Solidi a* **62** 483–93
- [9] Grüner G and Zettl A 1985 *Phys. Rep.* **119** 117–232
- [10] Flemming R, Moncton D and McWhan D 1978 *Phys. Rev. B* **18** 5560–3
- [11] Sweetland E, Tsai C-Y, Wintner B A, Brock J D and Thorne R E 1990 *Phys. Rev. Lett.* **65** 3165–8
- [12] McCarten J, DiCarlo D A, Maher M P, Adelman T L and Thorne R E 1992 *Phys. Rev. B* **46** 4456–82
- [13] Zaitsev-Zotov S V, Pokrovskii V Y and Monceau P 2001 *JETP Lett.* **73** 25–7
- [14] Zaitsev-Zotov S V 2003 *Microelectron. Eng.* **69** 549–54

- [15] Slot E, van der Zant H S J, O'Neill K and Thorne R E 2004 *Phys. Rev. B* **69** 73105
- [16] Slot E, Holst M A, Van Der Zant H S J and Zaitsev-Zotov S V 2004 *Phys. Rev. Lett.* **93** 1–4
- [17] Stabile A A, Whittaker L, Wu T L, Marley P M, Banerjee S and Sambandamurthy G 2011 *Nanotechnology* **22** 485201
- [18] Hor Y S, Xiao Z L, Welp U, Ito Y, Mitchell J F, Cook R E, Kwok W K and Crabtree G W 2005 *Nano Lett.* **5** 397–401
- [19] Mantel O, Chalin F, Dekker C, van der Zant H, Latyshev Y, Pannetier B and Monceau P 2000 *Phys. Rev. Lett.* **84** 538–41
- [20] Thompson A, Zetl A and Grüner G 1981 *Phys. Rev. Lett.* **47** 64–7
- [21] Fleming R M 1980 *Phys. Rev. B* **22** 5606–12
- [22] Lee P and Rice T 1979 *Phys. Rev. B* **19** 3970–80
Allender D, Bray J W and Bardeen J 1974 *Phys. Rev. B* **9** 119
Rice M J 1974 *Low-Dimensional Cooperative Phenomena* ed H J Keller (New York: Plenum) p 23
- [23] Bardeen J, Ben-Jacob E, Zetl A and Grüner G 1982 *Phys. Rev. Lett.* **49** 493–6
- [24] Brazovskii S, Kirova N, Requardt H, Nad F, Monceau P, Currat R, Lorenzo J, Grübel G and Vettier C 2000 *Phys. Rev. B* **61** 10640–50
- [25] Isakovic A F, Evans P G, Kmetko J, Cicak K, Cai Z, Lai B and Thorne R E 2006 *Phys. Rev. Lett.* **96** 1–4